Electron Microscopic and Optical Diffraction Analysis of the Structure of Scorpion Muscle Thick Filaments

ROBERT W. KENSLER,* RHEA J. C. LEVINE,*§ and MURRAY STEWART‡§
*Department of Anatomy, Medical College of Pennsylvania, Philadelphia, Pennsylvania 19129; ‡Medical Research Council Laboratory of Molecular Biology, Cambridge CB2 2QH, England; and §Pennsylvania Muscle Institute, University of Pennsylvania Medical School, Philadelphia, Pennsylvania 19104

ABSTRACT We rapidly and gently isolated thick filaments from scorpion tail muscle by a modification of the technique previously described for isolating *Limulus* thick filaments. Images of negatively stained filaments appeared to be highly periodic, with a well-preserved myosin cross-bridge array. Optical diffraction patterns of the electron micrograph images were detailed and similar to optical diffraction patterns from *Limulus* and tarantula thick filaments. Analysis of the optical diffraction patterns and computed Fourier transforms, together with the appearance of the filaments in the micrographs, suggested a model for the filaments in which the myosin cross-bridges were arranged on four helical strands with 12 cross-bridges per turn of each strand, thus giving the observed repeat every third cross-bridge level. Comparison of the scorpion thick filaments with those isolated from the closely related chelicerate arthropods, *Limulus* and tarantula, revealed that they were remarkably similar in appearance and helical symmetry but different in diameter.

Invertebrate muscle thick filaments are bipolar assemblies of the proteins myosin and paramyosin arranged so that the paramyosin forms a core covered by the myosin. Electron microscopic and biochemical studies have shown that the thick filaments from different phylogenetic groups are remarkably diverse in both their dimensions and paramyosin content (5–7, 9, 14, 16, 20, 21). In addition, x-ray diffraction studies of relaxed muscles from several different species revealed that, although all of the myosin cross-bridges in the thick filaments were helically arranged and projected from the filament backbone every 14.5 nm, there was considerable diversity in the screw symmetry of the myosin helix (2, 22–26). The factors controlling this diversity are at present unknown.

Recently we demonstrated by electron microscopy that the filaments of the chelicerate arthropods, *Limulus* and tarantula, were similar in structure (9, 15). Filaments from both species were periodic with a myosin helical pitch of 174 nm and had extremely similar arrangements of the myosin heads on the filament surface (9, 15, 17). These results suggested the possibility that the structure of the thick filaments in the chelicerate arthropods might be phylogenetically conserved. To investigate this hypothesis we examined the structure of thick filaments isolated from the relaxed muscles of another chelicerate arthropod, the scorpion, and we describe here the similarities and differences between these filaments and those of *Limulus* and tarantula, and also discuss the significance of these observations.

MATERIALS AND METHODS

Thick filaments were isolated from whole tail muscles of the scorpion *Vejovis spinigera* by a modification of the technique previously used to isolate *Limulus* and tarantula thick filaments (9, 15, 17). In this procedure animals anesthetized by cold were quickly killed and their excised tails were slit open to expose the muscles. The tails were immersed overnight in a mincing solution containing 0.1 M NaCl, 2 mM EGTA, 1 mM dithiothreitol, 5 mM $MgCl_2$, and 7 mM sodium phosphate buffer (pH 7) at 4°C. The muscle was then dissected free of the remaining pieces of the exoskeleton and homogenized in relaxing solution of the same composition as the mincing solution except that the NaCl was replaced with KCl and 2.5 mM ATP was added. Homogenization was performed on ice with two 15-s bursts (separated by 30 s) at setting 3 of a Sorvall OmniMixer (Du Pont Instruments–Sorvall Biomedical Div., Wilmington, DE) using the 5-ml cup. The homogenate was diluted with additional relaxing solution to 15 ml and centrifuged at 3,000 *g* for 10 min to pellet the large debris. Separated thick and thin filaments remained in the supernatant and were absorbed onto grids with thin carbon films (5–7 nm) supported by holey Formvar films. Negative staining was performed using either 1% uranyl acetate as previously described (9, 11) or a tannic acid-uranyl acetate procedure. In the latter procedure thick filaments absorbed to the carbon films were rinsed sequentially with eight drops each of relaxing solution, 0.25% tannic acid (Mallinckrodt Ar 1764; Mallinckrodt Inc., Science Products Div., St. Louis, MO) in 0.05 M ammonium acetate, 0.1 M ammonium acetate, and then negatively stained with 1% uranyl acetate. The tannic acid solution was prepared daily as a 0.5% stock which was diluted with an equal volume of 0.1

M ammonium acetate. In a few cases the filaments were absorbed to perforated Formvar films (stabilized with carbon) without an underlying thin carbon film and then negatively stained employing the tannic acid–uranyl acetate procedure. These latter grids were then further stabilized after staining by evaporation of a thin layer of carbon onto their surfaces (19, 20). *Limulus* and tarantula thick filaments were isolated as previously described (9, 15) and similarly stained.

For platinum or platinum–carbon shadowing, isolated filaments, absorbed to standard thickness carbon films on grids, were sequentially rinsed with eight drops each of relaxing solution, 0.1 M ammonium acetate, 1% uranyl acetate, and 10% glycerol. The grids were dried for 30–60 min under vacuum (pressure $\leq 10^{-5}$ torr) in a Denton DV 502 vacuum evaporator (Denton Vacuum Inc., Cherry Hill, NJ) to remove the glycerol. The uranyl acetate acts to stabilize the filaments against collapse during drying (10, 20), and the glycerol appears to improve the helical ordering of the cross-bridges (20). Shadowing of the filaments with platinum or platinum-carbon was performed as previously described (10) at a shadowing angle of 20–30° and a specimen-to-electrode distance of 15 cm.

Negatively stained and platinum-shadowed preparations were examined in either a JEOL 100S electron microscope or a Phillips 300 electron microscope with the anti-contamination device in operation. Magnification was calibrated using catalase crystals (27) or tropomyosin tactoids (1).

Optical diffraction, optical filtration, and computer image processing were performed as previously described (9, 10, 11, 17). Spacings on the diffraction patterns were calculated relative to the spacing ($1/14.5$ nm^{-1}) of the meridional reflection on the third layer line (23).

RESULTS

Negative Staining

Thick filaments isolated from freshly dissected scorpion tail muscles were negatively stained either with 1% uranyl acetate or with a tannic acid–uranyl acetate procedure which appeared to give higher contrast and better delineation of the cross-bridges. The appearance of the filaments stained by either procedure was strikingly periodic (Figs. 1–3), and similar to that of the thick filaments isolated from both *Limulus* and tarantula (9, 15). The filaments were 4–5 μm long, with distinct central bare zones (Fig. 1) and a bipolar appearance. On either side of the bare zone, the myosin cross-bridge pattern appeared to repeat (or have a near-repeat) every third level of cross-bridges (43.5 nm) with an axial spacing of 14.5 nm between adjacent cross-bridge levels. Careful inspection of the high magnification micrographs (Figs. 2 and 3) revealed that the cross-bridge pattern along the filament appeared bilaterally symmetrical, consistent with the myosin heads' being arranged along an even number of helical strands, such that the cross-bridges would project symmetrically from opposite sides of the filament at each cross-bridge level. This pattern appeared to extend uniformly along the arms of the filament, except at the bare zone and in the short tapered regions at the ends of the filaments. The maximum filament diameter, measured in the cross-bridge region of the tannic acid–uranyl acetate stained filaments, averaged 29.3 ± 2.2 nm (mean ± SD; $n = 350$). If the filament diameter in the bare zone (17.7 ± 1.6 nm mean ± SD; $n = 50$) is taken as representative of the filament backbone diameter, the myosin cross-bridges will project 5.8 nm from the filament shaft.

Optical Diffraction

We used optical diffraction analysis to confirm and analyze the periodicity of the filaments. Electron micrographs of the isolated thick filaments at a magnification of ~20,000 were diffracted in a laser optical diffractometer (4, 12). The electron micrographs of filaments stained with uranyl acetate alone gave strong optical diffraction patterns (Fig. 4), which showed a series of layer lines indexing as orders of a 43.5 nm helical repeat (Table I). Meridional reflections occurred on the third ($1/14.5$ nm^{-1}) and sixth ($1/7.2$ nm^{-1}) layer lines, and the entire pattern was consistent with the presence of a repeat in the helical structure every third cross-bridge level. The first and fourth layer lines were relatively strong, whereas the second and fifth were weak. Qualitatively, the patterns were very similar to x-ray diffraction patterns obtained from *Limulus* (25, 26) and tarantula (24) muscle and to the optical diffraction patterns obtained from filaments of these animals (9, 15). The patterns obtained from filaments stained with the uranyl acetate–tannic acid procedure were very similar but showed a slight deviation in the axial position of nonmeridional maxima from the values found using uranyl acetate alone (Table I). This deviation was most marked for the first layer line and resulted in the spacing of this layer line's corresponding to ~46 nm, which was >3 × 14.5 nm. These values may indicate a slightly longer pitch of the helices along which the cross-bridges lie in filaments stained with tannic acid–uranyl acetate, but this deviation would be relatively small, ~3–5%.

Using the argument $2\pi rR = 3.8$ to describe the position of the first subsidiary peak of the zero-order Bessel functions, which contribute to the meridional reflection on the third layer line and the measured radial spacing (R in the above equation) of the subsidiary peak (Table I; see references 8, 25, and 26), we calculated that the cross-bridges were centered at a radius (r) of ~12.8 nm in the uranyl acetate-stained filaments and ~11.4 nm in the tannic acid–treated filaments. Using this calculated radius and the radial position of the primary maxima on the first layer line (Table I) in the two sets of patterns, we estimated the number of helical strands (N) on which the cross-bridges lie. The primary maximum on this layer line is derived from a sum of Bessel functions of order N (represented by J_N), where N is the number of helical strands (13). A Bessel function of order 4 has a maximum when $2\pi rR = 5.32$, which is close to the values of $2\pi rR = 5.12$ calculated for the uranyl acetate stained filaments and 5.34 calculated for the filaments pretreated with tannic acid (Table I). A Bessel function of order 3 would have a maximum when $2\pi rR = 4.2$, whereas a Bessel function of order 5 would have a maximum at 6.4. Thus, the radial position of the maxima on the layer line strongly supports a four-stranded arrangement of the myosin heads on the surface of the scorpion thick filaments.

Computer Image Processing

We obtained further support for a four-stranded arrangement by examining the phases of the primary maxima in computed Fourier transforms of digitized electron micrographs of the scorpion thick filaments. These maxima will be in phase for an even number of strands but 180° out of phase for an odd number (13). In all filaments examined (7 stained with uranyl acetate only and 10 stained with tannic acid-uranyl acetate) the phase difference between these reflections was never >20° and was usually <10°. This confirmed that there was an even number of strands and effectively eliminated three- and five-stranded models.

Platinum Shadowing

The scorpion filaments, like *Limulus* and tarantula filaments (10, 15), showed a right-handed helical arrangement of

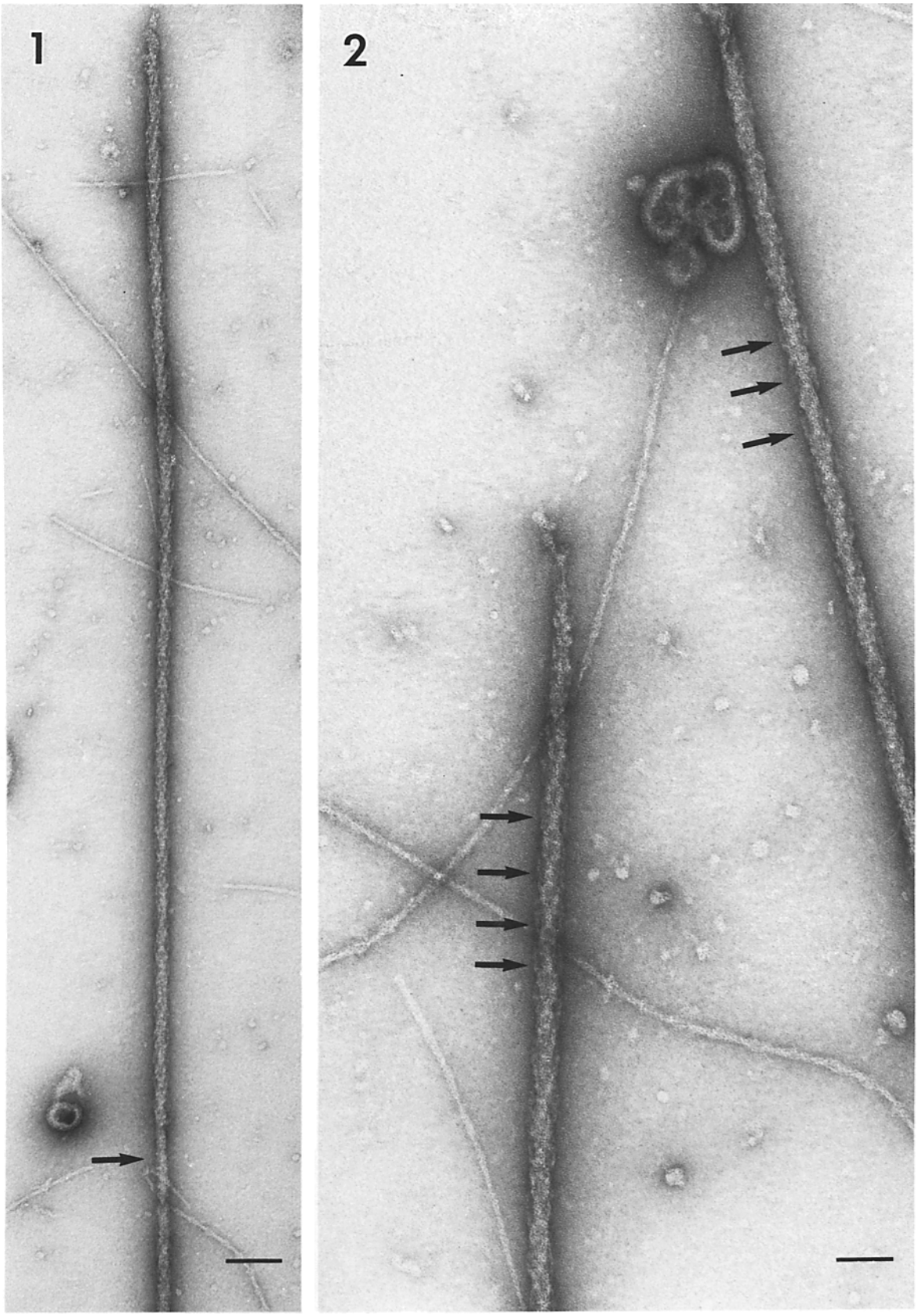

FIGURES 1 and 2 Low and medium magnification electron micrographs of isolated scorpion muscle thick filaments negatively stained by the tannic acid–uranyl acetate procedure. Fig. 1 illustrates the long length and central bare zone (arrow) of the filaments. In Fig. 2 the extremely periodic arrangement of the myosin cross-bridges along the filament is illustrated. Areas in which the cross-bridges appear to project from both sides of the backbone at the same cross-bridge level are indicated (Fig. 2, arrows). Note the apparent bilaterally symmetrical appearance of the cross-bridge arrangement on either side of the filament axis. The adjacent thinner filaments in both figures are the actin-containing thin filaments. Fig. 1: bar, 100 nm; × 92,000. Fig. 2: bar, 50 nm; × 184,000.

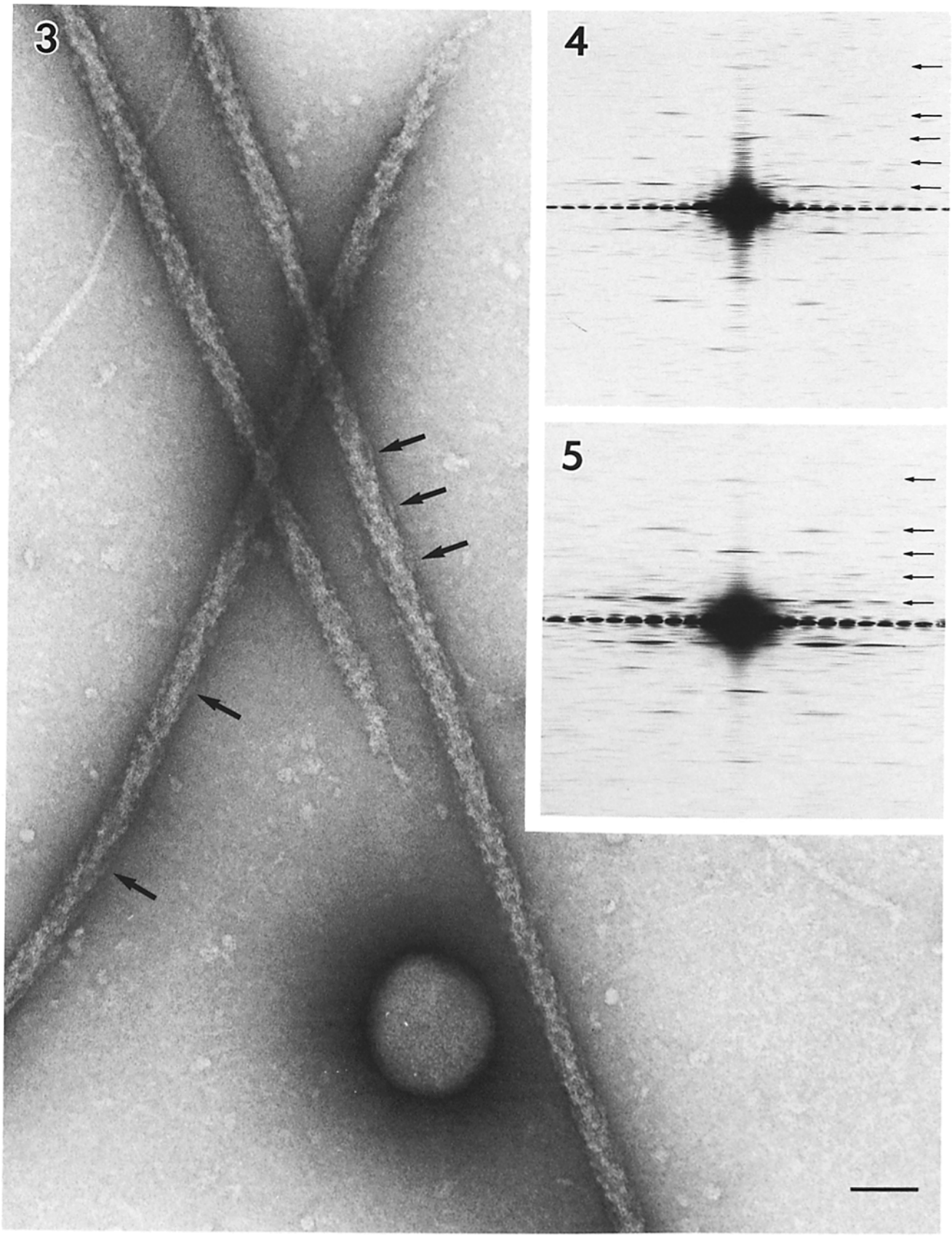

FIGURES 3–5 Fig. 3: A high magnification electron micrograph of isolated scorpion thick filaments negatively stained by the tannic acid-uranyl acetate procedure. Note the highly periodic appearance of the cross-bridge pattern along the filament and the numerous places (arrows) in which cross-bridges can be seen projecting from opposite sides of the backbone at the same cross-bridge level. Bar, 50 nm. × 250,000. Figs. 4 and 5: Optical diffraction patterns obtained from electron micrograph images of filaments negatively stained either with uranyl acetate alone (Fig. 4) or by the tannic acid-uranyl acetate procedure (Fig. 5). The arrows in both figures indicate the approximate positions of the strongest layer lines in the patterns. Note the close similarity in appearance of the two diffraction patterns and the high degree of periodic order of the cross-bridges indicated by the strength of the patterns. Note that the slight splitting of the meridional maxima on the third and sixth layer lines in pattern 4 (uranyl acetate alone) is not typical.

TABLE I. *Optical Diffraction Pattern Measurements and Calculations*

Staining method	Uranyl acetate (alone)	Tannic acid-uranyl acetate
	$1/nm^{-1}$	$1/nm^{-1}$
Layer line spacings		
1	43.8 ± 2.1* (16)‡	45.6 ± 1.8 (35)
2	21.7 ± 0.46 (16)	21.5 ± 0.5 (28)
3	14.5 (standard)	14.5 (standard)
4	10.9 ± 0.17 (16)	11.0 ± 0.12 (35)
5	—	—
6	7.3 ± 0.08 (15)	7.2 ± 0.11 (30)
Radial spacings of diffraction maxima on layer lines (LL)		
Primary on first LL	15.7 ± 2.4 (16)	13.4 ± 1.6 (35)
Primary on fourth LL	15.6 ± 1.4 (16)	13.9 ± 1.7 (30)
First subsidiary, third LL	21.1 ± 3.2 (12)	18.9 ± 2.6 (28)
Calculated cross-bridge radius§	12.8 nm	11.4 nm
Computed argument ($2\pi rR$) for position of primary maxima on first LL (R in nm^{-1})	5.12	5.34
Expected table values: $J_3 = 4.2$, $J_4 = 5.32$, $J_5 = 6.4$		

All spacings in the diffraction pattern were calculated relative to the spacing of the third LL meridional reflection, which was assigned a value of 1/14.5 nm^{-1}.

* Mean ± SD.

‡ Numbers in parentheses indicate number of diffraction patterns measured.

§ Based on equation $r = (3.8/2\pi R)$, where R is the radial spacing of first subsidiary maxima on third LL expressed in nanometers^{-1}.

subunits on their surfaces (Figs. 6 and 7) when unidirectionally shadowed with platinum. These subunits were best delineated on filaments oriented almost parallel to the direction of shadowing, whereas in filaments oriented almost perpendicular to the shadowing direction the helical striations appeared as almost continuous ridges of density (Figs. 6 and 7). The helical strands extended uniformly across both arms of the filament except at the bare zone, which is consistent with the interpretation that the subunits were the myosin heads. Six or seven subunits could routinely be counted along each half-turn of the helical strands, as expected for a four-stranded arrangement of the cross-bridges. Optical diffraction patterns of the filaments showing well-delineated subunits were qualitatively very similar to those from negative-stained filaments but were dominated by reflections arising from only the upper surface of the filaments (Fig. 8).

DISCUSSION

The results presented here demonstrate that scorpion thick filaments can be isolated under relaxing conditions with their myosin cross-bridges arranged in a highly ordered helical array, as shown by the detailed images and optical diffraction patterns we routinely obtained. The filaments appeared strikingly similar to *Limulus* and tarantula thick filaments previously observed (3, 9, 10, 15, 17). The negatively stained and platinum-shadowed filaments from all three species showed well-ordered right-handed helical arrays of cross-bridges that had a helical repeat (or near-repeat) every third cross-bridge level (43.5 nm) with an axial spacing of 14.5 nm between cross-bridge levels.

Comparison of optical diffraction patterns obtained from electron micrograph images of the scorpion filaments stained with uranyl acetate with those obtained previously from similarly stained *Limulus* (9, 10, 17) and tarantula filaments (15) confirmed this similarity in the helical symmetry of the cross-bridges. Diffraction patterns from all three species revealed a series of layer lines indexing close to the expected orders of a 43.5-nm helical repeat. Meridional reflections were present on the third and sixth layer lines, indicating three-fold screw symmetry for the filaments from all three animals. The patterns from all three filaments were also similar in showing strong first and fourth layer lines and weak second and fifth layer lines. Wray et al. (25) have interpreted this feature in x-ray diffraction patterns of *Limulus* as indicating that the cross-bridge was probably curved and aligned roughly along the direction of the long pitch helical strand. Three-dimensional reconstructions of *Limulus* filaments (17) support this interpretation, and a similar interpretation may hold for scorpion (18) and tarantula filaments (3).

The calculations presented here based upon optical diffraction patterns and computed Fourier transforms strongly support a four-stranded helical model for the scorpion thick filament, in good agreement with similar calculations performed for *Limulus* and tarantula thick filaments (9, 15) and with computer image reconstruction studies of these latter filaments (3, 17). The analysis of the phase difference between the primary maxima on the first layer line of the transforms obtained by computer image analysis virtually eliminated the possibility of three-stranded and five-stranded helical models for the scorpion thick filament. A four-stranded model for the scorpion filaments was further supported by the images of the platinum-shadowed filaments, which showed the presence of 6 or 7 subunits per half-turn of the helix, consistent with the 12 subunits per turn expected for a four-stranded helix with three-fold screw symmetry and a helical repeat every third crossbridge level. The results were thus consistent with the thick filaments from all three animals having a similar arrangement of the myosin cross-bridges along four helical strands.

The striking similarity in the surface cross-bridge lattice on the thick filaments of scorpion, tarantula, and *Limulus* is intriguing because these animals are closely related phylogenetically and represent the major classes of the chelicerate arthropods. The results suggest that the surface lattice of the thick filaments may be phylogenetically conserved in these arthropods, whereas the organization of the cross-bridges of many other arthropod thick filaments is quite different (22–26) and may even vary among the thick filaments of different muscles of the same animal (22, 23). Within the scorpion tail and leg muscles and in *Limulus* telson muscle, we have observed that, although by phase microscopy more than one fiber type may be present (Kensler, R. W., and R. J. C. Levine, unpublished observation), by electron microscopy all of the filaments observed appear to have the same cross-bridge arrangement. At present the functional significance (if any) of this conservation of cross-bridge arrangement in the chelicerate arthropods is unclear, although it may reflect some highly conserved feature of the geometry of the interactions of paramyosin and myosin coiled coils.

Although similar, the thick filaments from scorpion, tarantula, and *Limulus* do vary in diameter and paramyosin/

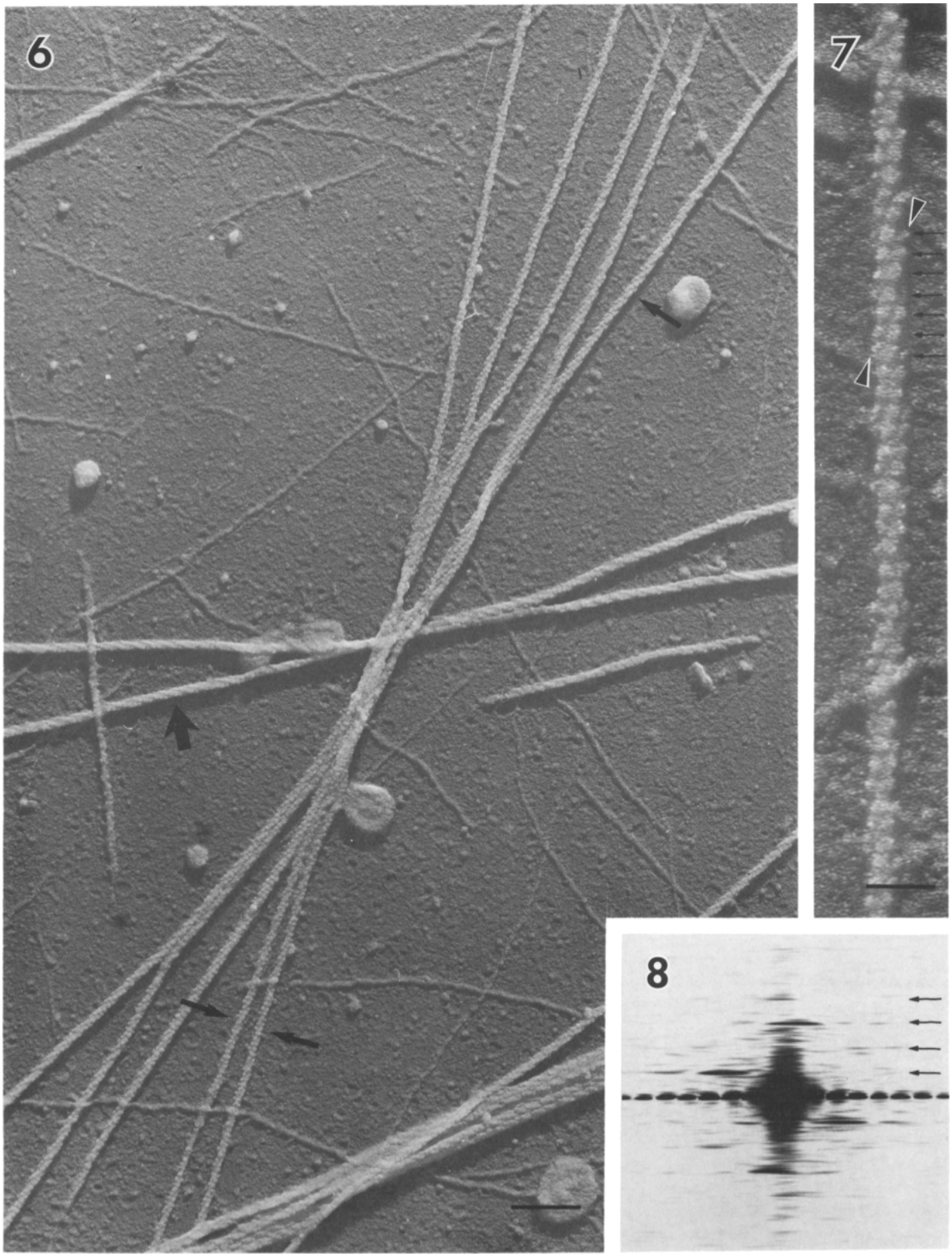

FIGURES 6–8 Figs. 6 and 7: Low and high magnification electron micrographs of scorpion filaments unidirectionally shadowed with platinum-carbon. Fig. 6 shows a field of filaments in which the long length and periodic appearance of the filaments are apparent. Note that filaments aligned with their axes almost parallel to the direction of shadowing display well-delineated subunits that lie along right-handed helical tracks (small arrows), whereas filaments (large arrow) oriented more perpendicular to the direction of shadowing display a more ropelike appearance with less delineation of the subunits. The appearance of the subunits is apparent in Fig. 7, where it can be seen that six or seven subunits (arrows) occur along the helical track indicated between the arrowheads. Fig. 6: bar, 200 nm; × 60,000. Fig. 7: bar, 50 nm; × 250,000. Fig. 8: An optical diffraction pattern obtained from the image of a platinum-carbon shadowed filament similar to that shown in Fig. 7. The arrows indicate the layer lines that occur at spacings that correspond to a helical repeat distance of 43.5 nm.

myosin ratios. Scorpion filaments are somewhat smaller in diameter (29.3 nm) than are the filaments from *Limulus* muscle (40 nm) (9). Based upon their diameter in thin sections and in negatively stained images, tarantula filaments also appear to be smaller in diameter than do *Limulus* filaments (15). This difference in diameter is probably reflected in the smaller calculated radii at which the cross-bridges are centered in scorpion (11.4–12.8 nm) and tarantula (13.4 nm) filaments (15) than in *Limulus* filaments (15.5 nm) (9). In addition, tarantula filaments have a lower paramyosin-to-myosin heavy chain ratio (0.31) than is found (0.48) for *Limulus* thick filaments (14, 15). Preliminary work also suggests that the scorpion filaments have a lower paramyosin-to-myosin heavy chain ratio (Levine, R. J. C. unpublished observation). Although, in a previous study of a variety of invertebrate muscles, Levine et al. (14) found little correlation between the paramyosin content and the diameter among "classes" of thick filaments that were structurally very different from each other, in the present case it is tempting to speculate that the smaller diameter of the scorpion and tarantula filaments may be correlated with a lower paramyosin-to-myosin ratio. This speculation is supported by the smaller diameter of the scorpion and tarantula bare zones (17.7 and 19–20 nm, respectively) than of *Limulus* thick filaments (24 nm), which would be consistent with these otherwise very similar filaments, having a paramyosin core of smaller diameter. Furthermore, as a consequence of their different diameters, the circumference of *Limulus*, scorpion, and tarantula thick filament shafts will not be the same. Therefore, not only will the circumferential separation of myosin heads be greater, but the myosin tails will also be further apart in the filaments that have greater shaft diameters, which implies that there is some difference in the packing of the myosin tails and paramyosin in the different filament types. This could come about, for example, by the thicker myosin filaments' having more paramyosin between the myosin tails on the surface; alternatively, if the myosin tails were located partially on the surface and partially in the bulk of the filament shaft, the fraction of the tail on the surface could change.

At present the role of the paramyosin in the invertebrate thick filament, other than to act as a core for the filament, is not well understood. Nor are the factors that determine the helical arrangement of the myosin on the filament surface. The thick filaments of the chelicerate arthropods, however, because of their similarity (but not identity) in structure may provide a model system for studying the factors that determine cross-bridge arrangement. As an initial step in this direction, we examined the structure of both scorpion and *Limulus* thick filaments by further computer image analysis. The results of these studies are presented in the accompanying paper (18).

We thank Dr. P. Chantler for helpful discussion, and Ruth Bingler and Harriet King for laboratory and photographic assistance.

This work was supported by U. S. Public Health Service grants AM30442 to Dr. Kensler and HL15835 to the Pennsylvania Muscle Institute.

A preliminary report of part of this work was presented at the Annual Meeting of the Biophysical Society, Boston, MA, 14–17 February 1982 (Kensler, R. W., R. J. C. Levine, M. Reedy, and W. Hoffmann. 1982. *Biophys. J.* 37(2, Pt. 2):34*a*. [Abstr.]).

Received for publication 3 December 1984, and in revised form 22 April 1985.

REFERENCES

1. Caspar, D. L. D., C. Cohen, and W. Longley. 1969. Tropomyosin: crystal structure, polymorphism, and molecular interactions. *J. Mol. Biol.* 41:87–97.
2. Castellani, L., P. Vibert, and C. Cohen. 1983. Structure of myosin/paramosin filaments from a molluscan smooth muscle. *J. Mol. Biol.* 167:853–872.
3. Craig, R., and R. Padron. 1982. Structure of tarantula muscle thick filaments. *J. Muscle Res. Cell Motil.* 3:487. (Abstr.)
4. DeRosier, D. J., and A. Klug. 1972. Structure of tubular variants of the head of bacteriophage T_4 (polyheads). I. Arrangement of subunits in some classes of polyheads. *J. Mol. Biol.* 65:469–488.
5. Dewey, M. M., R. J. C. Levine, and D. E. Colflesh. 1973. Structure of *Limulus* striated muscle. The contractile apparatus at various sarcomere lengths. *J. Cell Biol.* 58:574–593.
6. Elfvin, M., R. J. C. Levine, and M. M. Dewey. 1976. Paramyosin in invertebrate muscles. I. Identification and localization. *J. Cell Biol.* 71:261–272.
7. Elliot, A., and P. Bennett. 1982. Structure of the thick filaments in molluscan adductor muscle. *In*: Basic Biology of Muscles: A Comparative Approach. B. M. Twarog, R. J. C. Levine, and M. M. Dewey, editors. Raven Press, New York. 11–28.
8. Haselgrove, J. C. 1980. A model of myosin crossbridge structure consistent with the low angle x-ray diffraction pattern of vertebrate muscle. *J. Muscle Res. Cell Motil.* 1:177–191.
9. Kensler, R. W., and R. J. C. Levine. 1982. An electron microscopic and optical diffraction analysis of the structure of *Limulus* telson muscle thick filaments. *J. Cell Biol.* 92:443–451.
10. Kensler, R. W., and R. J. C. Levine. 1982. Determination of the handedness of the crossbridge helix of *Limulus* thick filaments. *J. Muscle Res. Cell Motil.* 3:349–361.
11. Kensler, R. W., and M. Stewart. 1983. Frog skeletal muscle thick filaments are three-stranded. *J. Cell Biol.* 96:1797–1802.
12. Klug, A., and J. E. Berger. 1964. An optical method for the analysis of periodicities in electron micrographs and some observations on the mechansim of negative staining. *J. Mol. Biol.* 10:565–569.
13. Klug, A., F. H. C. Crick, and H. W. Wyckoff. 1958. Diffraction by helical structures. *Acta Crystallogr.* 11:199–213.
14. Levine, R. J. C., M. Elfvin, M. M. Dewey, and B. Walcott. 1976. Paramyosin in invertebrate muscles. II. Content in relation to structure and function. *J. Cell Biol.* 71:273–279.
15. Levine, R. J. C., R. W. Kensler, M. C. Reedy, W. Hofmann, and H. A. King. 1983. Structure and paramyosin content of tarantula thick filaments. *J. Cell Biol.* 97:186–195.
16. Millman, B., and P. Bennett. 1976. The structure of a cross-striated molluscan muscle: the adductor muscle of the scallop. *J. Mol. Biol.* 103:439–467.
17. Stewart, M., R. W. Kensler, and R. J. C. Levine. 1981. Structure of *Limulus* telson muscle thick filaments. *J. Mol. Biol.* 153:781–790.
18. Stewart, M., R. W. Kensler, and R. J. C. Levine. 1985. Three-dimensional reconstruction of thick filaments from *Limulus* and scorpion muscle. *J. Cell Biol.* 101:402–411.
19. Taylor, K. A., and L. A. Amos. 1981. A new model for the geometry of the binding of myosin crossbridges to muscle thin filaments. *J. Mol. Biol.* 147:297–324.
20. Vibert, P., and R. Craig. 1983. Electron microscopy and image analysis of myosin filaments from scallop striated muscle. *J. Mol. Biol.* 165:303–320.
21. Winkelman, L. 1976. Comparative studies of paramyosins. *Comp. Biochem. Physiol.* 55B:391–397.
22. Wray, J. S. 1979. Structure of the backbone in myosin filaments of muscle. *Nature (Lond.).* 277:37–40.
23. Wray, J. S. 1979. X-ray diffraction studies of myosin filament structures. *In*: Motility in Cell Function. F. A. Pepe, J. W. Sanger, and V. T. Nachmias, editors. Academic Press, Inc., New York. 347–350.
24. Wray, J. S. 1982. Organization of myosin in invertebrate thick filaments. *In* Basic Biology of Muscle: A Comparative Approach. B. M. Twarog, R. J. C. Levine, and M. M. Dewey, editors. Raven Press, New York. 29–36.
25. Wray, J. S., P. J. Vibert, and C. Cohen. 1974. Crossbridge arrangements in *Limulus* muscle. *J. Mol. Biol.* 88:343–348.
26. Wray, J. S., P. J. Vibert, and C. Cohen. 1975. Diversity of crossbridge configurations in invertebrate muscles. *Nature (Lond.).* 257:561–564.
27. Wrigley, N. G. 1968. The lattice spacing of crystalline catalase as an internal standard of length in electron microscopy. *J. Ultrastruct. Res.* 24:454–464.